https://doi.org/10.5194/egusphere-2026-1881
Preprint. Discussion started: 18 May 2026

Codominant tree species showcase opposing hydraulic capacitance-reliance in Central Texas

Caleb Earl Adams[1,2], Ashley M. Matheny[2], Suvan A. Cabraal[3], Sanna Sevanto[1], Adam Atchley[1]

[1]Earth and Environmental Science Division, Los Alamos National Laboratory, Los Alamos, New Mexico, 87545, USA

[2]Department of Earth and Planetary Sciences, Jackson School of Geosciences, University of Texas at Austin, Austin, Texas, 78712, USA

[3]Bureau of Economic Geology, Jackson School of Geosciences, University of Texas at Austin, Austin, Texas, 78758, USA

Correspondence to: Caleb Earl Adams (ceadams@lanl.gov)

Abstract. Understanding the stress-responses of the tree species that comprise ecosystems is important for making predictions of how those ecosystems will respond to future stress events, e.g., drought. Past work has shown differential reliance on hydraulic capacitance, water released from internal storage, to maintain daily transpiration and gas-exchange with the atmosphere. In this study, we used wavelet coherence analysis to quantify the relationship between water supply (soil moisture), atmospheric water demand (VPD), and tree-water measurements (wood water content and sap flow) for two codominant tree species in a Central Texas woodland, escarpment live oak (*Quercus fusiformis*) and Ashe juniper (*Juniperus ashei*), over one and a half years including a period of extreme drought. Wavelet coherence provides a measure of correlation between the periodicity of signals at different frequencies or periods. The goal of our study was to analyze how the study trees' responses to environmental moisture conditions changed over time, especially during drought conditions. Our results revealed that, for both species, vapor pressure deficit and sap flow were strongly correlated at the 24-hour period, even during severe drought. Wood water content, especially for *Q. fusiformis,* was strongly correlated with soil moisture at daily to weeks-long periods. Our results also showed that vapor pressure deficit had a strong, and sustained, correlation with *Q. fusiformis* wood water content at the 24-hour period as drought severity increased, while *J. ashei* wood water content did not have this same relationship to vapor pressure deficit. Our results suggested that both species continue daily transpiration during severe drought, and that *Q. fusiformis* is more reliant on capacitance than *J. ashei* to maintain daily transpiration leading up to, and during, severe drought conditions. This difference in drought response strategy has important implications for each species' survival through shifting hydroclimatic conditions.

1. Introduction

Plant hydraulic responses to environmental conditions associated with water availability are critical to predicting plant-water status, drought-induced mortality, and the potential vulnerability and risk of wildfire (Ding et al., 2025; Ma et al., 2021; Powell et al., 2017) as well as understanding exchanges of carbon, water, and energy between the land and the atmosphere (Bonan, 2015). Over the last 45 years, atmospheric evaporative demand has caused a 40% global increase in the severity of droughts (Gebrechorkos et al., 2025; Vicente-Serrano et al., 2022), which have resulted in widespread tree mortality and landscape-level vegetation change due to plant-water stress or combined disturbances (Breshears et al., 2005; Crouchet et al., 2019; Fauset et al., 2012; Feeley et al., 2012).

Trees respond to their environment according to species-specific traits and behaviors. The traits and behaviors that determine how trees access, move, and store water comprise a plant's hydraulic strategy which includes rooting characteristics, stomatal regulation, and xylem architecture (Matheny et al., 2017b). Water moves through the soil-plant-atmosphere continuum along a water potential (MPa) gradient; as water evaporates from stomatal openings at the leaf surface, water held in tension within the tree is pulled upward from roots through the xylem and finally to the leaf. As tension increases (i.e., water potentials become increasingly negative), air bubbles can form in xylem vessels

https://doi.org/10.5194/egusphere-2026-1881
Preprint. Discussion started: 18 May 2026

(Tyree and Sperry, 1989). This process, known as embolism, causes a blockage which reduces overall hydraulic conductance. Some species of tree can buffer the effect of very negative water potential by utilizing capacitance, defined as the amount of water released from storage per change in water potential; capacitance can come from different sources within the stem including embolized vessels (Hölttä et al., 2009; Scholz et al., 2011). Coexisting species within an ecosystem often have different or opposing hydraulic strategies (Matheny et al., 2017a; Mcculloh et al., 2012; Pappas et al., 2018). Such diversity in species traits and behaviors can add to overall forest resilience (Fauset et al., 2012; Pappas et al., 2018). However, these differences also mean that some species may be more vulnerable to certain disturbances, depending on hydraulic strategy and species-specific responses to the environmental conditions that characterize the disturbance, and thus influence the ecosystem-level outcome (Brienen et al., 2015; Feeley et al., 2012; Matheny, 2021).

Ecosystems may exhibit stronger reliance on either vapor pressure deficit (VPD) or soil moisture, given vegetation type, species composition, or environmental conditions (Kibler et al., 2025; Novick et al., 2016; Sulman et al., 2016). Understanding vegetation sensitivity and responses to the environment is a complex problem given the natural interdependence among many controlling variables, such as solar radiation, temperature, VPD, and soil moisture. Furthermore, the dynamics of changing soil moisture and VPD fluctuations frequently operate at different timescales. Soil dries slowly over days and weeks, while VPD can change rapidly on the scale of minutes and hours. Yet both follow general trends over diurnal and seasonal periods. As hot droughts and VPD are expected to increase (AghaKouchak et al., 2021; Allen et al., 2015; Vicente-Serrano et al., 2022), it is critical to understand how forests, and the species that comprise them, respond to these stimuli in order to make predictions of vegetation moisture dynamics and ecosystem transition. Ecosystem-scale measurements such as those from eddy covariance flux towers and remote sensing products, can reveal how whole ecosystems rely on VPD or soil moisture (Kibler et al., 2025; Novick et al., 2016; Sulman et al., 2016). However, given the reliance of plant responses on species-specific traits and behaviors, species with opposing hydraulic strategies within an ecosystem can respond differently to changing weather patterns, leading to, for example, different drought-induced mortality rates. The seasonality and inherent differences across timescales of environmental conditions, along with plant responses across those timescales, present a challenge to disentangling relationships between environment and plant function that cannot be answered by linear regression alone. Rather, a time series analysis that detects time-lagged plant responses to environmental conditions, and how those responses change over time is needed.

Wavelet analysis, a signal processing technique, may provide new insights into how the relationships between plant-water and environmental moisture conditions change over time and across timescales. Wavelet transformation allows visualization of a one-dimensional timeseries in two-dimensional time-frequency, or time-period, space. In doing so, the frequencies, or timescales, at which a signal is strongest and how this strength changes over time are revealed. Wavelet transforms have been used in a wide range of Earth science studies, including examining how vegetative fluxes vary across timescales (Katul et al., 2001), how environmental factors control carbon assimilation in ecosystems (Stoy et al., 2005, 2009), and how environmental factors control water storage in an individual tree (Harmon et al., 2021). Wavelet coherence analysis offers a unique way to analyze the correlation between periodicities present in signals and to calculate time lags between those signals. In this study, we use wavelet coherence to compare how two codominant tree species in a semi-arid woodland respond to atmospheric demand and available soil moisture. While wavelet analysis alone is insufficient to identify the mechanisms behind the relationships we are studying (Stoy et al., 2005), it can nevertheless provide new insights into how these relationships change over time. The central goal of this analysis is to identify times when VPD or soil moisture dominates the control of plant hydraulic functions, and the timescales at which these controls occur.

This study aims to understand and disentangle the influences of VPD and soil moisture controls on vegetation hydrodynamics between two coexisting species with specific emphasis on uncovering how water stored in biomass (i.e., hydraulic capacitance) buffers the demands of these two forcings. We expect that trees with different hydraulic strategies will differ in their responses to these two drivers of the soil-plant-atmosphere continuum and that the

https://doi.org/10.5194/egusphere-2026-1881
Preprint. Discussion started: 18 May 2026

timescales of these responses will be determined by the timescales at which the environmental moisture dynamics change.

Our study site, on the Edwards Plateau in Central Texas, showcases opposing hydraulic strategies in the oft codominant species *Quercus fusiformis* (escarpment live oak), a diffuse porous angiosperm, and *Juniperus ashei* (Ashe juniper), a tracheid-bearing gymnosperm (Johnson et al., 2018a; Northup et al., 2022). Because VPD follows a predictable daily pattern and drives transpiration, we hypothesized that VPD will be correlated with sap flow in both species at the diel (24-hour) period. However, we expected that the species may stop transpiring as soil moisture decreases and drought severity increases, leading to a disruption in the diel correlation between VPD and sap flow signals, and that *J. ashei* sap flow will become less correlated with VPD sooner than *Q. fusiformis* during times of low soil moisture based on the findings of Northup et al (2022). If drought did not lead to a disruption of diel correlation, one explanation could be that the trees are utilizing capacitance to maintain transpiration. Thus, we also expected that, during drought, wood water content would be more correlated – as quantified by wavelet coherence – with VPD at the diel period, as we expected that the trees may be more reliant on their internal water stores to feed the daily transpiration stream. Given the longer timescales over which soil moisture changes, we expected wood water content and sap flow to be correlated to soil moisture at longer timescales.

2. Methods

2.1. Site and Data description

All tree data were collected at the White Family Outdoor Learning Center (WFOLC) located near Dripping Springs, TX on the Edwards Plateau (30°07'54"N 98°07'07"W). The Edwards Plateau in Central Texas is prone to frequent meteorological, hydrological, and hot droughts, including the exceptional drought of 2011 which resulted in widespread tree mortality (Crouchet et al., 2019; Klockow et al., 2018; Moore et al., 2016). The study site is characterized by very shallow soils (less than 10 cm) underlain by fractured limestone bedrock. It receives an average of 852 mm of precipitation annually and is considered a semi-arid woodland. Average temperatures range from 5º C in the winter to 38º C in the summer (Weather Underground, 2024).

The site is dominated by *Q. fusiformis* and *J. ashei*. *Q. fusiformis* is a diffuse porous species with xylem that are relatively vulnerable to cavitation and has been characterized as drought avoidant, which it may achieve by accessing alternative water sources rather than through stomatal closure (Northup et al., 2022). In contrast, *J. ashei* is a conifer with narrow cavitation-resistant tracheid and has been characterized as desiccation tolerant (Johnson et al., 2018b; McElrone et al., 2004; Northup et al., 2022). *Q. fusiformis* has also been found to root deeper into the fractured limestone bedrock than co-located *J. ashei* (Jackson et al., 1999), which potentially helped reduce drought mortality rates in *Q. fusiformis* during the notable 2011 drought (Northup et al., 2022). However, we do not have any measurements of rooting depths at our study site, and both species are known to root several meters into fractured bedrock.

Volumetric wood water content (WWC, $m^3\ m^{-3}$) was calculated from dielectric permittivity observations from capacitance-style soil moisture sensors (TEROS 12, METER Group Inc., Pullman, WA, USA) using calibration equations for each species derived according to the methods of Matheny et al. (2017). Sap flow (SF) measurements ($g\ s^{-1}$) were made using custom built Granier-style thermal dissipation sap flow sensors (Granier, 1986; Matheny et al., 2014). Raw sap flow data were filtered by removing measurements outside the expected thermocouple voltage range (0.2–0.8 mV), periods of sensor drift due to degradation, and anomalous spikes. Measurements were calibrated according to Oishi et al. (2016). Each of these measurements were made every fifteen minutes throughout the January 2022 to December 2024 study period (CR6 Datalogger, Campbell Scientific, Logan, UT, USA). Sensors were installed at breast height (~1.37m) on the north face of seven mature *Q. fusiformis* and six *J. ashei* located within a ~40m radius of one another. Average diameters at breast height (DBH) were 27.1 cm and 13.5 cm for *Q. fusiformis* and *J. ashei*,

https://doi.org/10.5194/egusphere-2026-1881
Preprint. Discussion started: 18 May 2026

respectively. Sap flow and volumetric wood water content were then averaged across individuals of each species at each timestep.

Vapor pressure deficit (VPD, kPa) data were collected from the Dripping Springs RAWS meteorological station, about 10.6 km from the study site (RAWS USA Climate Archive State Selection Map, 2025). For soil moisture, we used the 0-10 cm estimates from the NLDAS remote sensing package (NLDAS Get Data | LDAS, 2026) since the actual soil depth at the site rarely exceeds 10 cm in depth. This soil moisture estimate is modeled based on precipitation and a parameterized soil moisture model (Xia et al., 2014).

2.2. Cross-wavelet transform coherence

To test how sap flow and WWC responses to VPD and soil moisture changed over time, we used cross-wavelet transform coherence to analyze the relationships between signals in time-period space. For example, a high coherence value at the diel period between VPD and WWC would indicate that the daily release and refill of WWC is highly correlated to the diel pattern of VPD, thus indicating that capacitance was utilized to supply the transpiration stream. Similarly, a high diel coherence between VPD and sap flow would indicate that transpiration is highly correlated to the diel pattern of VPD, thus stomata are open throughout the day. Cross-wavelet transform coherence is an appropriate timeseries analysis method given the different timescales at which VPD and soil moisture operate and the expected tree response time (Grinsted et al., 2004). A wavelet transform (W_x) of a time series (x) is a convolution of the time series with a wavelet function, ψ. This convolution is performed for each timestep, and at several scales, which relate to frequency and are determined according to the sampling frequency of the time series. In this way, a one-dimensional (time) time-series is transformed into two-dimensional (time-period) space, revealing information about the frequencies – or periodicities – of the signal and how they change with time. In this work, we used the complex, continuous Morlet wavelet for extracting information from time series because it has a good balance between time and frequency resolution (Grinsted et al., 2004).

Continuous wavelet transforms were calculated for all the environmental (i.e. VPD, soil moisture) and plant-water (i.e. species-specific SF and WWC) time series using the Wavelet Toolbox in MATLAB. It is recommended that wavelet transforms be used on data that is at least near-normally distributed (Grinsted et al., 2004; Torrence and Compo, 1998). This is not the case for our data. VPD and SF data had gamma-like distributions, while WWC and soil moisture had multimodal distributions. Probability distributions were fit using a distribution fitting function in MATLAB. All data were transformed into records of percentiles using their respective distributions' cumulative density functions as recommended by Grinsted et al (2004). This resulted in distributions with a more rectangular shape. All time-series were then standardized to zero-mean and unit-variance.

We calculated cross-wavelet coherences (L_{xy}) as a measure of correlation between wavelet transforms of environmental and species-specific plant-water time series. Thus, the value of the cross-wavelet coherence at a given time and period represents how correlated the periodicities of the signals are at that period, at that particular time. In the following equation, x represents environmental time series, VPD and soil moisture, and y represents plant-water time series, SF and WWC:

$$L_{xy}(a,b) = \frac{\left|\sum_m W_x(a,b) W_y^*(a,b)\right|^2}{\left|\sum_m W_x(a,b)\right| \left|\sum_m W_y(a,b)\right|} \quad (1)$$

Where $*$ denotes the complex conjugate, a is representative of the period variable, and b represents the time variable. The parameter m is the number of time-steps used in smoothing the coherence. The value of m has implications for significance testing for the wavelet coherence (Ge, 2008). For our analysis, we set m as a function of frequency such that for any given period the coherence is given as an average coherence over 5 of those periods (e.g., at the 24-hour period, coherence is a 5-day average). Significance testing was performed using the wavelet coherence significance

https://doi.org/10.5194/egusphere-2026-1881
Preprint. Discussion started: 18 May 2026

test described by Ge (2008), with a significance level of 0.05. A total of eight cross-wavelet coherences were performed: two species, two plant-water time series, and two environmental time series.

For areas in the time-period space of high and significant coherence, we calculated the phase angles, from which we can calculate the time lags between the environmental drivers (VPD and SM) and plant-water responses. The phase angle, in radians, is given by

$$\theta = \arctan\left[\frac{\Im\left(W_{xy}(a,b)\right)}{\Re\left(W_{xy}(a,b)\right)}\right] + \mu\pi \quad (2)$$

Where $\Im$ and $\Re$ are the imaginary and real part, respectively. And $\mu = 0$ when the cross-wavelet transform, $W_{xy}(a,b) = W_x(a,b)W_y^*(a,b)$, is in the first or fourth quadrant of the complex plane, $\mu = 1$ when $W_{xy}(a,b)$ is in the second quadrant, and $\mu = -1$ when it's in the third quadrant. The phase angle, $-\pi \leq \theta \leq \pi$, represents a time lag between the two signals. A phase angle of 0 means the two signals are in phase, and a phase angle of $|\theta| = \pi$ means the two signals are in antiphase. Lag times, Δt, were then be calculated as follows:

$$\Delta t = \frac{\theta T}{2\pi} \quad (3)$$

Where T is the period (hours) for which the time lag is being calculated. A negative Δt implies that x (i.e., VPD or soil moisture) leads y (i.e., sap flow or WWC), while a positive Δt implies the opposite.

Cross-wavelet coherence gives no indication of the magnitude of signals. For example, we cannot tell from comparing cross-wavelet coherence values if sap flow is higher in either species at any given time.

2.3. Multivariate linear regression

We performed a multivariate linear regression analysis to assess the magnitude of the relative contributions of VPD and soil moisture to the variation in SF and WWC in *J. ashei* and *Q. fusiformis* following a procedure similar to Sulman et al (2016). Unlike Sulman et al (2016), who modeled the ratios of transpiration to a thirteen-year average, we had a more limited dataset. Thus, we calculated the ratios of SF/SF_{max} to obtain relative sap flow. The statistical models were fit for six conditions, low, middle, and high conditions for both soil moisture and VPD, as

$$\frac{SF}{SF_{max}} = C_1 + C_2 \ln(VPD) + C_3\Psi_{soil} + C_4 \ln(VPD) \times \Psi_{soil}, \quad (4)$$

Where Ψ_{soil} (MPa) is the soil water potential. Soil water potential was used since it is more representative, than soil water content, of the water available for root-water uptake within the soil-plant-atmosphere continuum (Sulman et al., 2016), and gave better results in the models. To calculate Ψ_{soil} from soil moisture, we used the Clapp-Hornberger water retention curve using parameters from the NLDAS soil map ($b = 8.17, \Psi_{sat} = 0.263, \theta_s = 0.465$). The natural logarithm of VPD was used following the example of Sulman et al (2016) and based on previous studies showing a linear relationship between stomatal conductance and ln (VPD) (Oren et al., 1999). All linear regression models were performed with the robust linear model, a least squares model that reduces the effects of outliers, in the Statsmodel Python package (Seabold and Perktold, 2010).

2.4. Keetch-Byram Drought Index

https://doi.org/10.5194/egusphere-2026-1881
Preprint. Discussion started: 18 May 2026

We calculated the Keetch-Byram Drought Index (KBDI) to characterize drought severity. We then analyzed how tree-water measurements, and their wavelet coherence with VPD and SM, evolve with drought severity. The KBDI ranges from 0 to 800, is used to monitor drought severity (higher values correspond to more severe drought), and is analogous to soil moisture deficit. It is calculated daily from precipitation, air temperature, and the previous day's KBDI. According to the Wildland Fire Assessment System (Keetch-Byram Drought Index, 2025) KBDI between 600 and 800 is associated with severe drought and live fuels that contribute to intense fire. McCaw et al (McCaw et al., 2018a) found that KBDI above 500 corresponded to critically low foliar moisture in *J. ashei* at sites on the Edwards Plateau.

3. Results

3.1. Wavelet coherence of WWC

Q. fusiformis water storage was more responsive to atmospheric moisture during dry soil moisture conditions than water storage of *J. ashei*, as seen by the longer durations of high coherence (Figure 1.a and b) for *Q. fusiformis* during the dry summer of 2023. For both species, high coherence between VPD and WWC were centered around the diel period (Figure 1.a and b). The summer of 2023 was an especially dry, hot summer with average daily high temperature of 38º C and average daily maximum VPD of 4.8 kPa. By July 15, 2023 KBDI reached 500, which is considered a threshold above which the foliar moisture content of *J. ashei* becomes critically low (McCaw et al., 2018a) and thus can be considered a time of water stress for the ecosystem. KBDI stayed at or above 500 through October 26, 2023. From May through October 2023, soil moisture ranged from a maximum of 0.42 m^3 m^{-3} to a minimum of 0.11 m^3 m^{-3}. The minimum soil moisture occurred on August 22. Both *Q. fusiformis* and *J. ashei* demonstrated durations of high coherence between WWC and VPD at the diel period during this hot, dry summer (Figure 3.b and c) with *Q. fusiformis* maintaining high coherence for longer durations. Both species also showed a long-term decrease in WWC during this summer, with *Q. fusiformis* WWC ranging from 0.38 m^3 m^{-3} in the spring to 0.23 m^3 m^{-3} on September 8, and *J. ashei* WWC ranging from 0.24 m^3 m^{-3} to 0.19 m^3 m^{-3} on September 13.

https://doi.org/10.5194/egusphere-2026-1881
Preprint. Discussion started: 18 May 2026

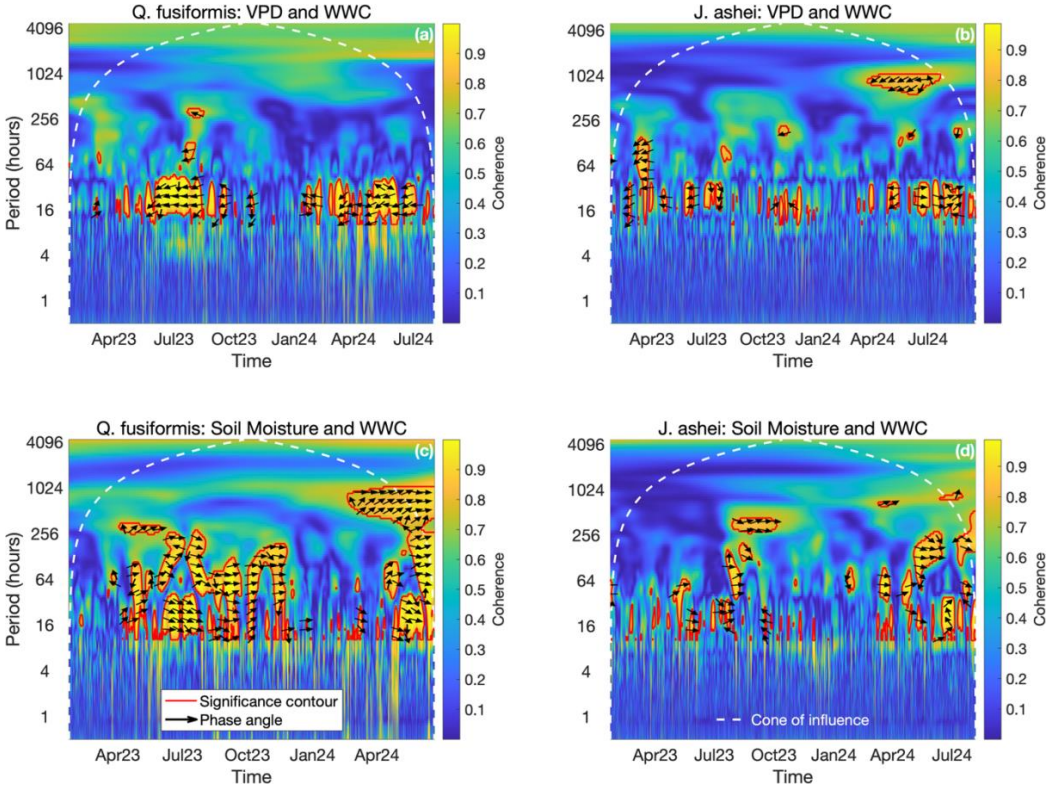

Figure 1: Wavelet coherence plots for (a) VPD and *Q. fusiformis* WWC, (b) VPD and *J. ashei* WWC, (c) soil moisture and *Q. fusiformis* WWC, and (d) soil moisture and *J. ashei* WWC. The closer the coherence is to 1, the more correlated the wavelet transforms of two time series are for a given period (y-axis) at a given moment in time (x-axis). The dashed white line indicates the cone of influence, outside of which wavelet coherence values are considered unreliable due to edge effects. The red contours show areas of significantly high coherence according to the significance test at a 0.05 significance level. The black arrows indicate the direction of the phase angle. If the arrow is pointing straight to the right, the phase angle at that time and period is 0; straight up means it's $\pi/2$; straight down means it's $-\pi/2$; straight left means $\pm\pi$. For both species, most of the high coherence of VPD and WWC is centered around the diel period at times of low soil moisture. This means that the diel cycles of WWC are highly correlated to the diel cycle of VPD at those times. Phase angle arrows mostly point to the left, indicating a phase angle near $-\pi$ meaning the signals are in antiphase. Overall, *Q. fusiformis* WWC signal is more correlated to the soil moisture signal at any period. Phase angle arrows show that soil moisture and WWC signals are often nearly in phase for both species.

The phase angles (Figure 1.a and b, black arrows) associated with the regions of high coherence around the diel period were mostly near $-\pi$ radians, indicating that the signals were in antiphase. By Eq. (3), this indicates that VPD reaches its daily maximum while WWC is around its daily minimum, then WWC has refilled as much as it is going to while VPD is reaching its daily minimum (time-lag of approximately 12h).

For both species, high coherence between soil moisture and WWC occurred during times of low soil moisture and at diel and longer periods. Between June 22 and August 22, 2023, soil moisture declined from 0.31 to 0.11 $m^3\ m^{-3}$ (Figure 3.f). By October 5, rains had increased soil moisture back to 0.36 $m^3\ m^{-3}$ (Figure 3.f). During this time of soil drying and subsequent rewetting, wavelet coherence was high at daily to weeks-long periods, especially for *Q. fusiformis* (Figure 1.c), suggesting that the *Q. fusiformis* water storage signal was more correlated to shallow soil moisture signal during dry conditions than *J. ashei* (Figure 1.d). The phase angles at the sub-daily to daily timescales during the summer of 2023 were near zero and negative, indicating that the signals were nearly in phase, with soil moisture

https://doi.org/10.5194/egusphere-2026-1881
Preprint. Discussion started: 18 May 2026

leading WWC (Figure 1.c and d; black arrows). Changes in WWC followed soil moisture closely during times of dry down (Figure 3.b and c). While *J. ashei* WWC had brief durations of coherence with soil moisture at the diel period leading up to the driest part of summer, as conditions reached their driest, the coherence shifted to longer periods (Figure 1.d), suggesting that the water content of *J. ashei* followed the long timescale trends of soil moisture as it dried. This agrees with the results in the time series plots – that *J. ashei* WWC dried with soil moisture but did not follow the soil moisture trend with the same fidelity as *Q. fusiformis* (Figure 3.b, c, and f).

3.2. Wavelet coherence of sap flow

In the wavelet coherence of VPD and sap flow of both species, significantly high coherence in the diel period existed for most of the study. The phase angles for both species were near zero at the diel period, indicating that VPD and sap flow were nearly in phase at the diel period. There were short breaks in the high coherence occurring at the end of summer 2023 and in January 2024. The break in coherence during summer 2023 was more pronounced for *J. ashei* (Figure 2.b) than for *Q. fusiformis* (Figure 2.a). For both species, this break in coherence occurred at the time when the KBDI reached its highest value of the season, indicating the drought was at its worst and soil moisture was very low (Figure 3.a). The breaks in coherence also coincided with precipitation events (Figure 3.d, e and f) and a decline in VPD (Figure 3.a), which likely indicated significant cloud cover during this period that would disrupt the diurnal pattern of VPD. The low coherence durations were longer and occurred more frequently for *J. ashei* than for *Q. fusiformis* (Figure 3.d and e).

https://doi.org/10.5194/egusphere-2026-1881
Preprint. Discussion started: 18 May 2026

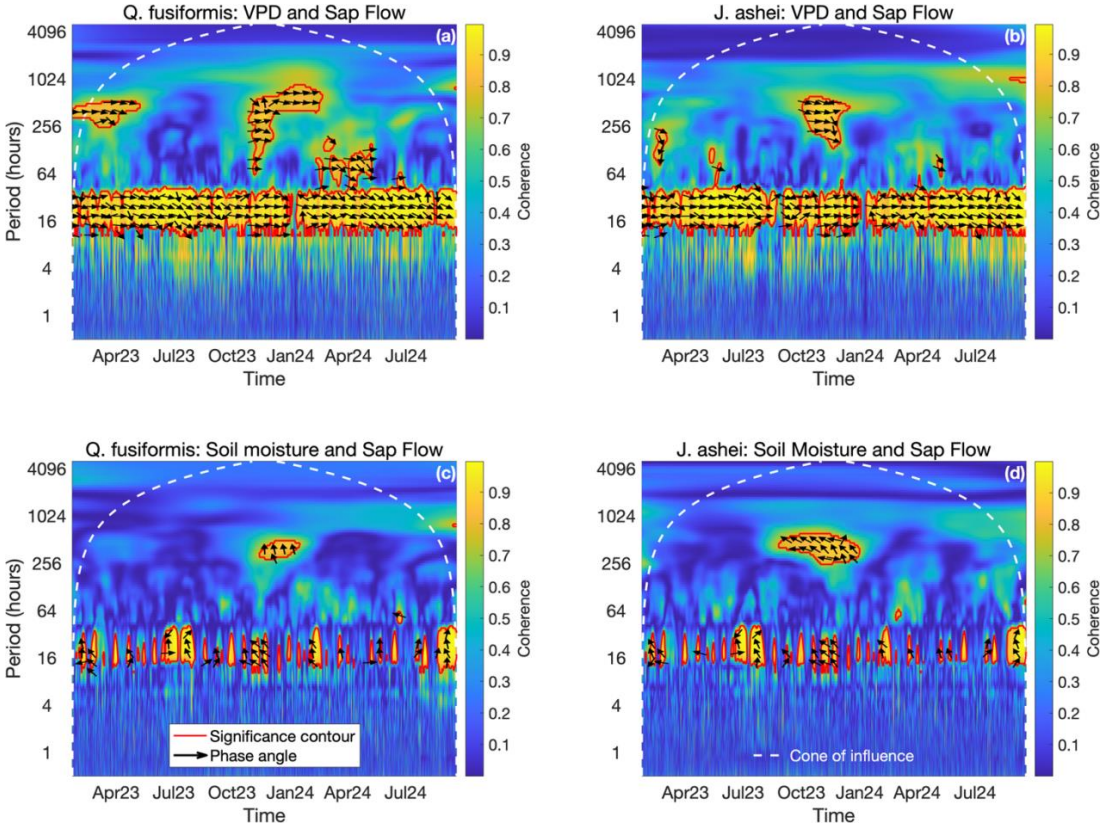

Figure 2: Wavelet coherence plots of (a) VPD and *Q. fusiformis* sap flow, (b) VPD and *J. ashei* sap flow, (c) soil moisture and *Q. fusiformis* sap flow, and (d) soil moisture and *J. ashei* sap flow. These plots demonstrate that both species have similar responses to both environmental conditions with respect to sap flow. Durations of high coherence between VPD and sap flow are centered around the diel period and are maintained for most of the study for both species, with some breaks in high coherence. Phase angles are close to in-phase and mostly negative, indicating that VPD leads sap flow. For soil moisture and sap flow, high coherence is centered around the diel period and is not consistent. When coherence is high, phase angles are mostly positive, indicating that sap flow leads soil moisture.

The durations of high coherence between soil moisture and sap flow centered at the diel period occurred at nearly the same times for both species. The positive values of the phase angles, evidenced by the upward direction of the arrows in Figure 2.(c and d), indicate that sap flow leads soil moisture. There was a strong diel coherence duration in the summer of 2023, suggesting a correlation between daily transpiration and soil drying patterns when conditions were hot and dry.

https://doi.org/10.5194/egusphere-2026-1881
Preprint. Discussion started: 18 May 2026

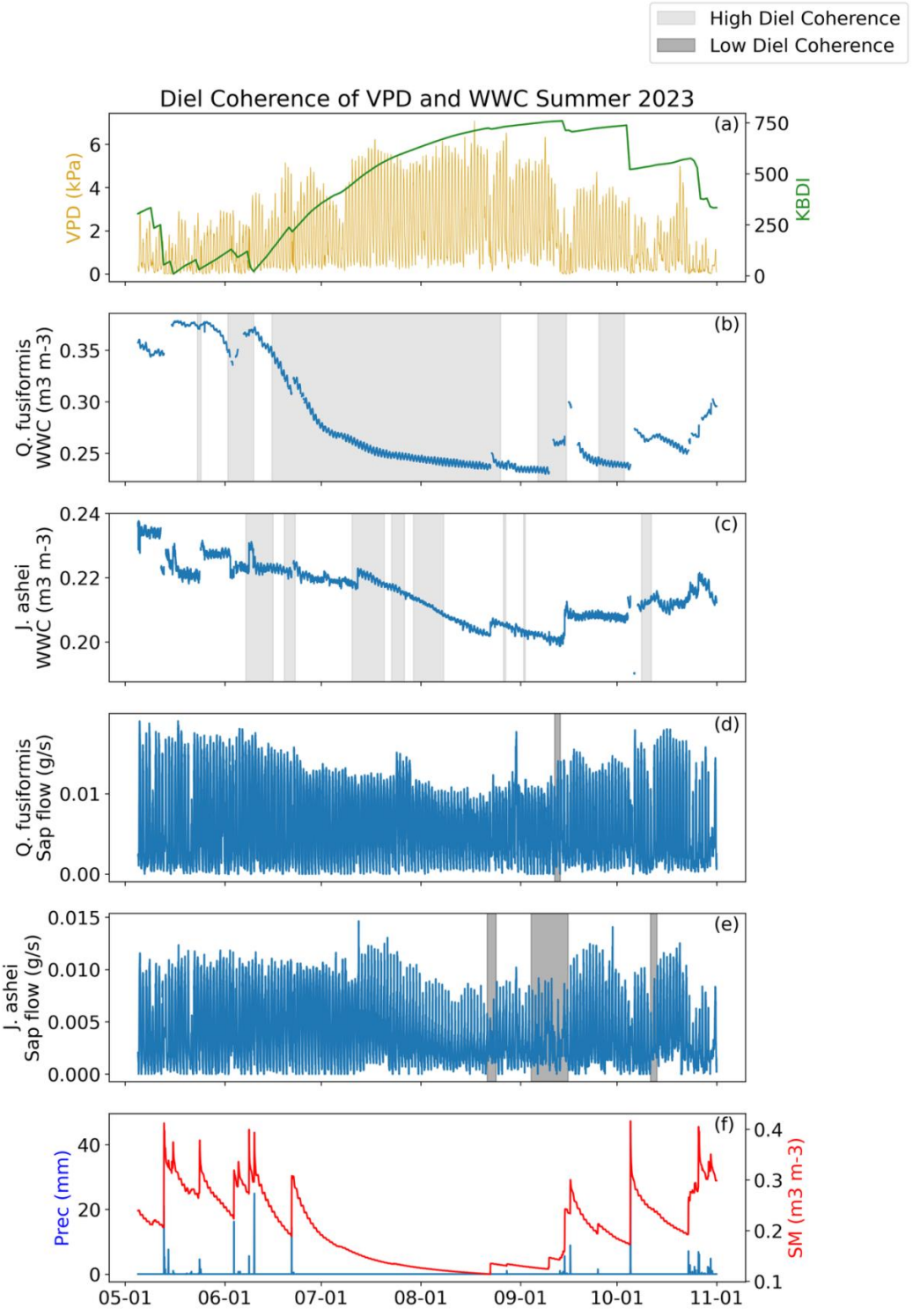

https://doi.org/10.5194/egusphere-2026-1881
Preprint. Discussion started: 18 May 2026

Figure 3: Meteorological conditions and sap flow time series from both species from May through October 2023. (a) VPD (kPa) and Keetch-Byram Drought Index; (b and c) wood water content for *Q. fusiformis* and *J. ashei*, respectively – the pink highlighted areas show times of high diel coherence between VPD and WWC for the respective species. *Q. fusiformis* (b) maintains high diel coherence for longer than *J. ashei* (c). (d and e) Sap flow for the two species – the purple highlighted regions represent times when diel coherence between VPD and sap flow becomes low. The drops in diel coherence are more pronounced for *J. ashei* (e) than *Q. fusiformis* (d) and coincide with days with low VPD and/or precipitation; (f) precipitation (mm) and shallow soil moisture (m^3m^{-3}).

3.3. Observed linear regression of Sap flow

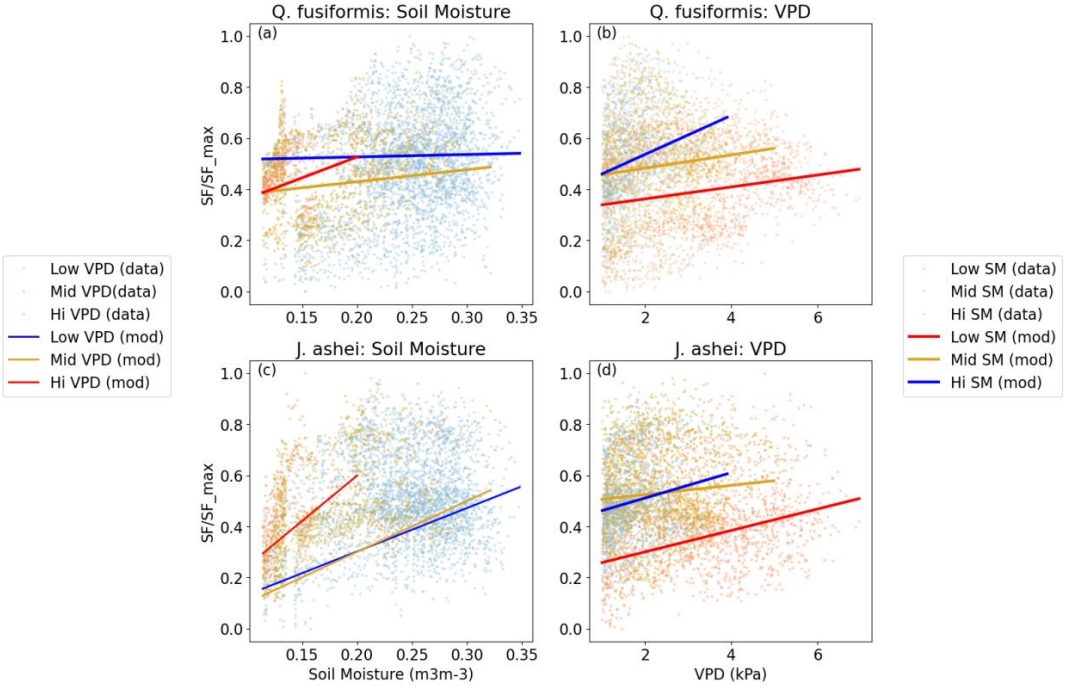

Figure 4: Robust linear regression of relative sap flow with VPD and Ψ_{soil} as independent variables. (a) Relative sap flow of *Q. fusiformis* as a function of soil moisture; (b) relative sap flow of *Q. fusiformis* as a function of VPD; (c) relative sap flow of *J. ashei* as a function of soil moisture; (d) relative sap flow of *J. ashei* as a function of VPD. In all plots, dots represent data points, and lines represent model predictions.

When soil moisture was low, both species maintained a positive relationship between sap flow and VPD. For both species, relative sap flow was most sensitive to VPD when soil moisture was high, as seen by the steeper slopes for high soil moisture compared to middle and low soil moisture (Figure 4.b and d), and by the high soil moisture coefficients on ln (VPD) of 0.2118 and 0.2350 ($p<0.001$) for *Q. fusiformis* and *J. ashei*, respectively, compared to 0.1032 and 0.1170 ($p<0.001$) for low soil moisture (Table 1 and 2). *J. ashei* was most sensitive to the interaction variable, $\ln(VPD) \times \Psi_{soil}$, with coefficient 0.9938 ($p=0.004$). Maximum sap flow ($SF_{\max}$, g s^{-1}) for the study period, used to calculate relative sap flow, was 0.0196 and 0.0130 for *Q. fusiformis* and *J. ashei,* respectively. This is about 50% higher for *Q. fusiformis* compared to *J. ashei*. Multiplying by $SF_{\max}$ for both species, absolute sap flow for *Q. fusiformis* was approximately 33% more sensitive to ln (VPD) than *J. ashei* with new coefficients of 0.0020 and 0.0015, respectively, suggesting that *Q. fusiformis* may be capable of greater sap flow rates with a stronger absolute response to VPD when soil moisture is low.

For both species, relative sap flow was most sensitive to Ψ_{soil} when VPD was high, with slopes on Ψ_{soil} of 0.0041 ($p<0.001$) and 0.0074 ($p<0.001$) at high VPD compared to 0.0013 ($p<0.001$) and 0.0024 ($p<0.001$) at low VPD for

https://doi.org/10.5194/egusphere-2026-1881
Preprint. Discussion started: 18 May 2026

Q. fusiformis and *J. ashei*, respectively (Table 1, Table 2). For all VPD levels, *J. ashei* relative sap flow was more sensitive to soil water potential than *Q. fusiformis* (Figure 4.a and c). However, for all VPD levels, relative sap flow was more sensitive to ln (VPD) than soil water potential, suggesting that VPD has stronger control over sap flow. Tables 1 and 2 provide a full description of linear model fit statistics.

Table 1: The variables and their coefficients from the linear regressions for relative sap flow of *Q. fusiformis*. A total of six models were made for six conditions: Low, Medium, and High VPD/SM

Q. fusiformis relative sap flow						
Variables	Condition	Coefficient	p-value	Condition	Coefficient	p-value
ln (VPD)	Low VPD	0.0750	<0.001	Low SM	0.1032	<0.001
	Mid VPD	0.1413	0.003	Mid SM	0.0596	0.001
	High VPD	-0.5307	<0.001	High SM	0.2118	<0.001
Ψ_{soil}	Low VPD	0.0013	<0.001	Low SM	-0.0007	<0.001
	Mid VPD	-0.0002	0.781	Mid SM	0.0278	0.013
	High VPD	0.0041	0.001	High SM	0.1558	0.474
$\ln(VPD) \times \Psi_{soil}$	Low VPD	-0.0011	0.003	Low SM	0.0005	0.001
	Mid VPD	0.0005	0.434	Mid SM	-0.0049	0.694
	High VPD	-0.0021	0.005	High SM	0.33745	0.307

Table 2: The variables and their coefficients from the linear regressions for relative sap flow of *J. ashei*. A total of six models were made for six conditions: Low, Medium, and High VPD/SM

J. ashei relative sap flow						
Variables	Condition	Coefficient	p-value	Condition	Coefficient	p-value
ln (VPD)	Low VPD	0.0696	<0.001	Low SM	0.1170	<0.001
	Mid VPD	0.2891	<0.001	Mid SM	0.0587	<0.001
	High VPD	-0.3868	0.069	High SM	0.2350	<0.001
Ψ_{soil}	Low VPD	0.0024	<0.001	Low SM	0.0014	<0.001
	Mid VPD	0.0004	0.604	Mid SM	-0.0337	0.001
	High VPD	0.0074	0.007	High SM	-0.6669	0.001
$\ln(VPD) \times \Psi_{soil}$	Low VPD	-0.0007	0.034	Low SM	-0.0002	0.162
	Mid VPD	0.0009	0.104	Mid SM	0.0134	0.251
	High VPD	-0.0036	0.024	High SM	0.9938	0.004

4. Discussion

4.1. The role of capacitance in buffering drought stress

Based on our results, *Q. fusiformis* was highly reliant on stem water stores when soil water became limiting, while *J. ashei* did not demonstrate the same reliance on water stores, but depended on other mechanisms to maintain function during drought. There is evidence of a continuum with trees on one end exhibiting vulnerable xylem and a reliance on stored water, and trees on the other end having more resistant xylem (Meinzer et al., 2009). The two species in the current study showcase the ends of this continuum. *Q. fusiformis* is classified as diffuse porous and has wider xylem vessels compared to *J. ashei,* which has primarily tracheid-based conductive tissue, leading to the *Quercus* species having greater water storage capacity (Figure 3.b and c; compare y-axes for WWC of both species). Another consequence of wider xylem vessels is that *Q.* fusiformis is more vulnerable to embolism; stem P50, i.e., the xylem tension at which 50% of conductance is lost, for *Q. fusiformis* is -1.8 MPa (Johnson et al., 2018a) and is -13.41 MPa for *J. ashei* (McElrone et al., 2004). Based on wavelet coherence, *Q. fusiformis* water stores were more responsive to the diel cycle of VPD than the water stores of *J. ashei* under low soil moisture (Figure 1.a and b). We hypothesized that both species would rely on internal water stores during drought, and we observed a decline in wood water content during drought for both species. However, *Q. fusiformis* was clearly utilizing stored water for its daily transpiration

https://doi.org/10.5194/egusphere-2026-1881
Preprint. Discussion started: 18 May 2026

needs far more than *J. ashei*, as evidenced by longer, sustained durations of diel coherence between WWC and VPD signals during times of low soil moisture (Figure 1.a). The high diel coherence between *Q. fusiformis* WWC and VPD, and the fact that the signals were in antiphase at the diel period, suggests that not only were the *Q. fusiformis* trees using their water stores throughout the day, but they were also able to refill them overnight enough to have a strong signal at the diel period.

Another source of water storage in *Q. fusiformis* could be in parenchyma cells that store non-structural carbon (NSC) and water. There is evidence that angiosperms with more vulnerable xylem vessels, that operate at smaller safety margins, contain more parenchyma as the starches and water stored in those cells would be necessary for embolism repair and refill, while there is no correlation between these measurements in gymnosperms (Kiorapostolou et al., 2019). *Q. fusiformis*, an angiosperm, has been recorded operating at a negative hydraulic safety margin, i.e., with water potentials below its P50 value (Johnson et al., 2018a). Theoretically, this would cause significant loss of conductance and embolism within the xylem network. A significant percentage of water released from storage to feed daily transpiration needs could come from embolized vessels (Tyree and Yang, 1990). A large proportion of water stored in the *Q. fusiformis* trees was released during the summer 2023 drought (Figure 3.b). If the capacitance comes from embolized vessels, this suggests that the trees are experiencing a fair amount of embolism as the drought continues. If reliance on capacitance during drought leads to embolism in *Q. fusiformis,* a greater amount of parenchyma could potentially aid in post-drought recovery.

Both species lost WWC during drought, following the same general drying trend as soil moisture, but *Q. fusiformis* WWC followed soil moisture with much more fidelity than *J. ashei* (Figure 3.b, c, and f). The shifts of high coherence between soil moisture and *J. ashei* WWC (Figure 1.d) to higher periods as the summer 2023 dry period persisted reflect the overall drying trend. *Q. fusiformis* WWC showed more dynamic behavior overall; this, together with the fidelity with which the *Quercus* water storage followed the soil moisture, was reflected in high coherence between soil moisture and *Q. fusiformis* WWC across sub-daily to weekly timescales (Figure 1.c).

It is possible that the *Q. fusiformis* WWC signal was more correlated to the shallow soil moisture than that of *J. ashei* (Figure 2.a and b) because its higher responsiveness to VPD at the diel period (Figure 1.a), which indicates greater use of capacitance, caused the *Q. fusiformis* WWC to dry out in a similar manner to the remote sensing soil moisture estimates (Figure 3.b and f). In contrast, *J. ashei* WWC was less responsive to VPD at the diel period (Figure 1.b), indicating that capacitance was not being used to the same extent as in *Q. fusiformis* and less connection between *J. ashei* WWC and the atmosphere. Thus, it could be that the differences of the wavelet coherence of soil moisture and WWC between the two species has more to do with capacitance use than rooting behavior. Currently, we do not have enough information about the subsurface at our study site, or the roots of the trees, to know the depths from which the study trees acquire water. We know that the soil is very shallow (~10 cm), and both species rely on water in the fractured bedrock, into which they are known to root several meters deep (Jackson et al., 1999). Thus, while the soil moisture estimates we used from the remote sensing product may be a good estimate of water in the shallow soil, it may not be representative of all the water available to the trees. A better understanding of the subsurface of our study site, the rooting behavior of the study trees, and how different roots contribute to transpiration and refill during drought (Grossiord et al., 2017; Nadezhdina and Cermak, 2000) would greatly improve our analysis.

4.2. Vapor pressure deficit is the dominant driver of tree water relations in this ecosystem

The consistent diel relationship between VPD and sap flow signals (Figure 2.a and b) suggests that both study species continued transpiration regardless of changes in drought severity, unlike species which stop transpiration under drought conditions such as piñon pine in New Mexico (Grossiord et al., 2017; Sevanto et al., 2018). Even when KBDI surpassed 500, a threshold above which *J. ashei* is likely to have critically low foliar moisture (McCaw et al., 2018b), both species maintained high coherence between VPD and sap flow (Figure 2.a and b). This contradicted our hypothesis that drought would lead to a break in coherence between VPD and sap flow. In fact, times when sap flow and VPD signals were not coherent appear to coincide with precipitation and low VPD events and were likely not

https://doi.org/10.5194/egusphere-2026-1881
Preprint. Discussion started: 18 May 2026

related to drought severity. Results from the linear regression showed a positive relationship between VPD and sap flow at all soil moisture levels, although VPD's effect on sap flow may be reduced when soil moisture is low (Figure 4; Table 1; Table 2). To maintain the relationship between diel cycles of VPD and sap flow, i.e., keep stomata open, when soil moisture is low the two species employed different strategies: *Q. fusiformis* showed a strong reliance on capacitance (Figure 1) as discussed in Section 4.1, while *J. ashei* likely reduces stomatal conductance, as found by Northup et al (2022), while not shutting its stomata completely. Wavelet coherence does not give magnitudes. Thus, it cannot show if one species is transpiring more than the other. The results from linear regressions suggest that *J. ashei* relative sap flow was more sensitive to VPD than *Q. fusiformis* relative sap flow under low soil moisture conditions (Table 1; Table 2), but further calculations (Section 3.3) showed that absolute sap flow of *Q. fusiformis* was more sensitive to VPD, and likely capable of higher rates, under low soil moisture. Both species are known to root several meters into fractured limestone bedrock (Jackson et al., 1999; McElrone et al., 2004). The observed relationship between VPD and sap flow is consistent with findings at other deep water-dependent ecosystems where evapotranspiration remains tightly coupled to atmospheric moisture as shallow soil moisture becomes depleted (Kibler et al., 2025).

4.3. Future drought predictions and implications for the study species

Temperature and evaporative demand in Texas are forecasted to increase in the near future, which will exacerbate the severity of droughts even without any decreases in overall precipitation. By 2026, average temperatures in Texas are expected to be 1º C warmer than the average of the last 30 years. Days over 100º F (~38º C) are projected to be four times more common than in the 1980s (Escobedo et al., 2024). What does this mean for species, like *Q. fusiformis* and *J. ashei*, which maintain coupling with VPD even as shallow soils dry out? Both study species are highly drought-adapted with opposing strategies for dealing with drought. None of the trees in our study experienced mortality, but our results highlight key differences in their strategies, and we can speculate on how these strategies might play out during exceptional droughts. Overall, *J. ashei* experienced greater mortality rates than *Q. fusiformis* as a result of the 2011 drought in Texas (Johnson et al., 2018a). Differences in mortality between the species were not consistent from site to site, and many factors were found to contribute that are not accounted for in this study (Crouchet et al., 2019).

Q. fusiformis may potentially be able to avoid drought stress and mortality by utilizing and refilling capacitance to maintain higher stomatal conductance for carbon uptake, especially at sites where it has access to deeper water. However, if the species were to experience prolonged drought characterized by increased temperatures and VPD, the aggressive water use strategy seen in the summer of 2023 could lead to significant, sustained loss of conductance. *Q. fusiformis* has been documented shedding leaves during drought(Northup et al., 2022),and we assume that stomata would eventually close, but the release of large proportions of water stores to the atmosphere early in a drought might cause irreparable damage if precipitation does not arrive on time. Crouchet et al. (2019) found that *Q. fusiformis* mortality from the 2011 drought was negatively correlated with stand density; if the relationship between VPD and the hydraulic systems of *Q. fusiformis* causes stress under drought conditions, the stress may be mitigated by the microclimate effects of denser stands, e.g., lower VPD and temperature.

J. ashei does not rely on capacitance in the same way as *Q. fusiformis* (Figure 1.a and b). *J. ashei* does release and refill water stores every day, and its water stores are lost over time when there is not adequate water available for refilling, but not to the same extent as its *Quercus* counterpart (Figure 1.a and b; Figure 3.b and c). Instead of capacitance, *J. ashei* relies on cavitation-resistant xylem (McElrone et al., 2004), stomatal regulation (Northup et al., 2022), and plasticity in leaf hydraulic traits (Johnson et al., 2018b) to maintain function during drought. Unlike *Q. fusiformis*, stand density was positively correlated with *J. ashei* mortality from the 2011 drought (Crouchet et al., 2019), potentially indicating that the effects of resource competition overcame any potential microclimate buffering. The different relationships between drought mortality and stand density between species could be due to how they access water, given that *Q. fusiformis* has been found to root deeper than *J. ashei* (Jackson et al., 1999).

5. Conclusions

https://doi.org/10.5194/egusphere-2026-1881
Preprint. Discussion started: 18 May 2026

Our analysis revealed that vapor pressure deficit was the main driver of tree-water relations for both *Q. fusiformis* and *J. ashei* regardless of drought severity, *Q. fusiformis* was more reliant on capacitance than *J. ashei* when soil moisture was low, and that *Q. fusiformis* WWC dynamics were more closely related to shallow soil moisture dynamics than those of *J. ashei*. The results of this study also highlight the importance of representing hydraulic capacitance in plant hydrodynamic models.

Given that both species remain responsive to VPD when shallow soil moisture is low, future droughts characterized by high temperatures and high VPD threaten ecosystems dominated by these species. At sites where trees have access to deeper water sources through fractured bedrock effects may be mitigated. However, both species also rely on water input via precipitation to refill internal water stores. Therefore, deep water access may not be enough to survive droughts that coincide with increased temperatures and VPD. This applies not only to the ecosystem in this study, but to other ecosystems that rely on deep water and maintain a strong connection to the atmosphere during drought.

Data and code availability

The Python and MatLab scripts used for analysis and visualization are available from the corresponding author upon request. Data used in the analysis is available here https://doi.org/10.5281/zenodo.19377015.

Author contributions

CA and AM: conceptualization of the study. SC and AM: data curation. CA: formal analysis, visualization, and writing (original draft preparation). AM, SS, and AA: supervision. All authors: writing (reviewing and editing).

Competing interests

The contact author has declared that none of the authors has any competing interests

Acknowledgements

The authors would like to acknowledge the White Family Outdoor Learning Center in Hayes county, Texas, where all data on the trees were collected. We would also like to thank all members, past and present, of the Matheny Ecohydrology Lab who worked diligently to set up and maintain the site.

Financial support

This material is based upon work supported by the U.S. Department of Energy, Office of Science, Office of Advanced Scientific Computing Research, Department of Energy Computational Science Graduate Fellowship under Award Number DE-SC0023112. This work was also partially funded by The Department of Defense through the Strategic Environmental Research and Development Program project RC25-0189 and supported by NSF EAR CAREER Award 2046768.

References

AghaKouchak, A., Mirchi, A., Madani, K., Di Baldassarre, G., Nazemi, A., Alborzi, A., Anjileli, H., Azarderakhsh, M., Chiang, F., Hassanzadeh, E., Huning, L. S., Mallakpour, I., Martinez, A., Mazdiyasni, O., Moftakhari, H., Norouzi, H., Sadegh, M., Sadeqi, D., Van Loon, A. F., and Wanders, N.: Anthropogenic Drought: Definition, Challenges, and Opportunities, Rev. Geophys., 59, e2019RG000683, https://doi.org/10.1029/2019RG000683, 2021.

Allen, C. D., Breshears, D. D., and McDowell, N. G.: On underestimation of global vulnerability to tree mortality and forest die-off from hotter drought in the Anthropocene, Ecosphere, 6, art129, https://doi.org/10.1890/ES15-00203.1, 2015.

Keetch-Byram Drought Index: https://www.wfas.net/index.php?option=com_content&view=article&id=86&Itemid=487, last access: 19 November 2025.

https://doi.org/10.5194/egusphere-2026-1881
Preprint. Discussion started: 18 May 2026

NLDAS Get Data | LDAS: https://ldas.gsfc.nasa.gov/nldas/nldas-get-data, last access: 19 January 2026.

RAWS USA Climate Archive State Selection Map: https://raws.dri.edu/index.html, last access: 19 November 2025.

Bonan, G.: Ecological Climatology: Concepts and Applications, 3rd ed., Cambridge University Press, Cambridge, https://doi.org/10.1017/CBO9781107339200, 2015.

Breshears, D. D., Cobb, N. S., Rich, P. M., Price, K. P., Allen, C. D., Balice, R. G., Romme, W. H., Kastens, J. H., Floyd, M. L., Belnap, J., Anderson, J. J., Myers, O. B., and Meyer, C. W.: Regional vegetation die-off in response to global-change-type drought, Proc. Natl. Acad. Sci., 102, 15144–15148, https://doi.org/10.1073/pnas.0505734102, 2005.

Brienen, R. J. W., Phillips, O. L., Feldpausch, T. R., Gloor, E., Baker, T. R., Lloyd, J., Lopez-Gonzalez, G., Monteagudo-Mendoza, A., Malhi, Y., Lewis, S. L., Vásquez Martinez, R., Alexiades, M., Álvarez Dávila, E., Alvarez-Loayza, P., Andrade, A., Aragão, L. E. O. C., Araujo-Murakami, A., Arets, E. J. M. M., Arroyo, L., Aymard C., G. A., Bánki, O. S., Baraloto, C., Barroso, J., Bonal, D., Boot, R. G. A., Camargo, J. L. C., Castilho, C. V., Chama, V., Chao, K. J., Chave, J., Comiskey, J. A., Cornejo Valverde, F., da Costa, L., de Oliveira, E. A., Di Fiore, A., Erwin, T. L., Fauset, S., Forsthofer, M., Galbraith, D. R., Grahame, E. S., Groot, N., Hérault, B., Higuchi, N., Honorio Coronado, E. N., Keeling, H., Killeen, T. J., Laurance, W. F., Laurance, S., Licona, J., Magnussen, W. E., Marimon, B. S., Marimon-Junior, B. H., Mendoza, C., Neill, D. A., Nogueira, E. M., Núñez, P., Pallqui Camacho, N. C., Parada, A., Pardo-Molina, G., Peacock, J., Peña-Claros, M., Pickavance, G. C., Pitman, N. C. A., Poorter, L., Prieto, A., Quesada, C. A., Ramírez, F., Ramírez-Angulo, H., Restrepo, Z., Roopsind, A., Rudas, A., Salomão, R. P., Schwarz, M., Silva, N., Silva-Espejo, J. E., Silveira, M., Stropp, J., Talbot, J., ter Steege, H., Teran-Aguilar, J., Terborgh, J., Thomas-Caesar, R., Toledo, M., Torello-Raventos, M., Umetsu, R. K., van der Heijden, G. M. F., van der Hout, P., Guimarães Vieira, I. C., Vieira, S. A., Vilanova, E., Vos, V. A., and Zagt, R. J.: Long-term decline of the Amazon carbon sink, Nature, 519, 344–348, https://doi.org/10.1038/nature14283, 2015.

Crouchet, S. E., Jensen, J., Schwartz, B. F., and Schwinning, S.: Tree Mortality After a Hot Drought: Distinguishing Density-Dependent and -Independent Drivers and Why It Matters, Front. For. Glob. Change, 2, https://doi.org/10.3389/ffgc.2019.00021, 2019.

Ding, J., McDowell, N., Bailey, V., Conroy, N., Day, D. J., Fang, Y., Kemner, K. M., Kirwan, M. L., Koven, C. D., Kovach, M., Megonigal, P., Morris, K. A., O'Meara, T., Pennington, S. C., Peixoto, R. B., Thornton, P., Weintraub, M., Regier, P., Sandoval, L., Machado-Silva, F., Stearns, A., Ward, N., and Wilson, S. J.: Modeling the mechanisms of coastal vegetation dynamics and ecosystem responses to changing water levels, Biogeosciences, 22, 6963–6978, https://doi.org/10.5194/bg-22-6963-2025, 2025.

Escobedo, J., Ott, C., and Dedrick, J.: 2024: Assessment of Historic and Future Trends of Extreme Weather in Texas, 2024.

Fauset, S., Baker, T. R., Lewis, S. L., Feldpausch, T. R., Affum-Baffoe, K., Foli, E. G., Hamer, K. C., and Swaine, M. D.: Drought-induced shifts in the floristic and functional composition of tropical forests in Ghana, Ecol. Lett., 15, 1120–1129, https://doi.org/10.1111/j.1461-0248.2012.01834.x, 2012.

Feeley, K. J., Rehm, E. M., and Machovina, B.: perspective: The responses of tropical forest species to global climate change: acclimate, adapt, migrate, or go extinct?, Front. Biogeogr., 4, https://doi.org/10.21425/F5FBG12621, 2012.

Ge, Z.: Significance tests for the wavelet cross spectrum and wavelet linear coherence, Ann. Geophys., 26, 3819–3829, https://doi.org/10.5194/angeo-26-3819-2008, 2008.

Gebrechorkos, S. H., Sheffield, J., Vicente-Serrano, S. M., Funk, C., Miralles, D. G., Peng, J., Dyer, E., Talib, J., Beck, H. E., Singer, M. B., and Dadson, S. J.: Warming accelerates global drought severity, Nature, 642, 628–635, https://doi.org/10.1038/s41586-025-09047-2, 2025.

https://doi.org/10.5194/egusphere-2026-1881
Preprint. Discussion started: 18 May 2026

Granier, A.: Evaluation of transpiration in a Douglas-fir stand by means of sap flow measurements, 1986.

Grinsted, A., Moore, J. C., and Jevrejeva, S.: Application of the cross wavelet transform and wavelet coherence to geophysical time series, Nonlinear Process. Geophys., 11, 561–566, https://doi.org/10.5194/npg-11-561-2004, 2004.

Grossiord, C., Sevanto, S., Dawson, T. E., Adams, H. D., Collins, A. D., Dickman, L. T., Newman, B. D., Stockton, E. A., and McDowell, N. G.: Warming combined with more extreme precipitation regimes modifies the water sources used by trees, New Phytol., 213, 584–596, https://doi.org/10.1111/nph.14192, 2017.

Harmon, R. E., Barnard, H. R., Day-Lewis, F. D., Mao, D., and Singha, K.: Exploring Environmental Factors That Drive Diel Variations in Tree Water Storage Using Wavelet Analysis, Front. Water, 3, https://doi.org/10.3389/frwa.2021.682285, 2021.

Hölttä, T., Cochard, H., Nikinmaa, E., and Mencuccini, M.: Capacitive effect of cavitation in xylem conduits: results from a dynamic model, Plant Cell Environ., 32, 10–21, https://doi.org/10.1111/j.1365-3040.2008.01894.x, 2009.

Jackson, R. B., Moore, L. A., Hoffmann, W. A., Pockman, W. T., and Linder, C. R.: Ecosystem rooting depth determined with caves and DNA, Proc. Natl. Acad. Sci., 96, 11387–11392, https://doi.org/10.1073/pnas.96.20.11387, 1999.

Johnson, D. M., Domec, J.-C., Carter Berry, Z., Schwantes, A. M., McCulloh, K. A., Woodruff, D. R., Wayne Polley, H., Wortemann, R., Swenson, J. J., Scott Mackay, D., McDowell, N. G., and Jackson, R. B.: Co-occurring woody species have diverse hydraulic strategies and mortality rates during an extreme drought, Plant Cell Environ., 41, 576–588, https://doi.org/10.1111/pce.13121, 2018a.

Johnson, D. M., Berry, Z., Baker, K., Smith, D., McCulloh, K., and Domec, J.-C.: Leaf hydraulic parameters are more plastic in species that experience a wider range of leaf water potentials, Funct. Ecol., 32, https://doi.org/10.1111/1365-2435.13049, 2018b.

Katul, G., Lai, C.-T., Schäfer, K., Vidakovic, B., Albertson, J., Ellsworth, D., and Oren, R.: Multiscale analysis of vegetation surface fluxes: from seconds to years, Adv. Water Resour., 24, 1119–1132, https://doi.org/10.1016/S0309-1708(01)00029-X, 2001.

Kibler, C. L., Quetin, G. R., and Trugman, A. T.: Evapotranspiration Sensitivity to Environmental Variability Provides a Window Into Subsurface Processes in the Soil-Plant-Atmosphere Continuum, J. Geophys. Res. Biogeosciences, 130, e2025JG009097, https://doi.org/10.1029/2025JG009097, 2025.

Kiorapostolou, N., Da Sois, L., Petruzzellis, F., Savi, T., Trifilò, P., Nardini, A., and Petit, G.: Vulnerability to xylem embolism correlates to wood parenchyma fraction in angiosperms but not in gymnosperms, Tree Physiol., 39, 1675–1684, https://doi.org/10.1093/treephys/tpz068, 2019.

Klockow, P. A., Vogel, J. G., Edgar, C. B., and Moore, G. W.: Lagged mortality among tree species four years after an exceptional drought in east Texas, Ecosphere, 9, e02455, https://doi.org/10.1002/ecs2.2455, 2018.

Ma, W., Zhai, L., Pivovaroff, A., Shuman, J., Buotte, P., Ding, J., Christoffersen, B., Knox, R., Moritz, M., Fisher, R. A., Koven, C. D., Kueppers, L., and Xu, C.: Assessing climate change impacts on live fuel moisture and wildfire risk using a hydrodynamic vegetation model, Biogeosciences, 18, 4005–4020, https://doi.org/10.5194/bg-18-4005-2021, 2021.

Matheny, A. M.: Stressors Reveal Ecosystems' Hidden Characteristics, J. Geophys. Res. Biogeosciences, 126, e2021JG006462, https://doi.org/10.1029/2021JG006462, 2021.

Matheny, A. M., Bohrer, G., Vogel, C. S., Morin, T. H., He, L., Frasson, R. P. de M., Mirfenderesgi, G., Schäfer, K. V. R., Gough, C. M., Ivanov, V. Y., and Curtis, P. S.: Species-specific transpiration responses to intermediate

https://doi.org/10.5194/egusphere-2026-1881
Preprint. Discussion started: 18 May 2026

disturbance in a northern hardwood forest, J. Geophys. Res. Biogeosciences, 119, 2292–2311, https://doi.org/10.1002/2014JG002804, 2014.

Matheny, A. M., Bohrer, G., Garrity, S. R., Morin, T. H., Howard, C. J., and Vogel, C. S.: Observations of stem water storage in trees of opposing hydraulic strategies, Ecosphere, 6, art165, https://doi.org/10.1890/ES15-00170.1, 2015.

Matheny, A. M., Fiorella, R. P., Bohrer, G., Poulsen, C. J., Morin, T. H., Wunderlich, A., Vogel, C. S., and Curtis, P. S.: Contrasting strategies of hydraulic control in two codominant temperate tree species, Ecohydrology, 10, e1815, https://doi.org/10.1002/eco.1815, 2017a.

Matheny, A. M., Mirfenderesgi, G., and Bohrer, G.: Trait-based representation of hydrological functional properties of plants in weather and ecosystem models, Plant Divers., 39, 1–12, https://doi.org/10.1016/j.pld.2016.10.001, 2017b.

McCaw, W. M., Grobert, D. M., Brown, S. B., Strickland, S., Thompson, G. A., Gillman, G., Ball, L. M., and Robinson, C. D.: Seasonal Patterns and Drivers of Ashe Juniper Foliar Live Fuel Moisture and Relevance to Fire Planning, Fire Ecol., 14, 50–64, https://doi.org/10.4996/fireecology.140150064, 2018a.

McCaw, W. M., Grobert, D. M., Brown, S. B., Strickland, S., Thompson, G. A., Gillman, G., Ball, L. M., and Robinson, C. D.: Seasonal Patterns and Drivers of Ashe Juniper Foliar Live Fuel Moisture and Relevance to Fire Planning, Fire Ecol., 14, 50–64, https://doi.org/10.4996/fireecology.140150064, 2018b.

Mcculloh, K. A., Johnson, D. M., Meinzer, F. C., Voelker, S. L., Lachenbruch, B., and Domec, J.-C.: Hydraulic architecture of two species differing in wood density: opposing strategies in co-occurring tropical pioneer trees, Plant Cell Environ., 35, 116–125, https://doi.org/10.1111/j.1365-3040.2011.02421.x, 2012.

McElrone, A. J., Pockman, W. T., Martínez-Vilalta, J., and Jackson, R. B.: Variation in xylem structure and function in stems and roots of trees to 20 m depth, New Phytol., 163, 507–517, https://doi.org/10.1111/j.1469-8137.2004.01127.x, 2004.

Meinzer, F. C., Johnson, D. M., Lachenbruch, B., McCulloh, K. A., and Woodruff, D. R.: Xylem hydraulic safety margins in woody plants: coordination of stomatal control of xylem tension with hydraulic capacitance, Funct. Ecol., 23, 922–930, https://doi.org/10.1111/j.1365-2435.2009.01577.x, 2009.

Moore, G. W., Edgar, C. B., Vogel, J. G., Washington-Allen, R. A., March, R. G., and Zehnder, R.: Tree mortality from an exceptional drought spanning mesic to semiarid ecoregions, Ecol. Appl., 26, 602–611, https://doi.org/10.1890/15-0330, 2016.

Nadezhdina, N. and Cermak, J.: Responses of sap flow rate along tree stem and coarse root radii to changes of water supply, in: The Supporting Roots of Trees and Woody Plants: Form, Function and Physiology, edited by: Stokes, A., Springer Netherlands, Dordrecht, 227–238, https://doi.org/10.1007/978-94-017-3469-1_22, 2000.

Northup, A. P., Keitt, T. H., and Farrior, C. E.: Cavitation-resistant junipers cease transpiration earlier than cavitation-vulnerable oaks under summer dry conditions, Ecohydrology, 15, e2337, https://doi.org/10.1002/eco.2337, 2022.

Novick, K. A., Ficklin, D. L., Stoy, P. C., Williams, C. A., Bohrer, G., Oishi, A. C., Papuga, S. A., Blanken, P. D., Noormets, A., Sulman, B. N., Scott, R. L., Wang, L., and Phillips, R. P.: The increasing importance of atmospheric demand for ecosystem water and carbon fluxes, Nat. Clim. Change, 6, 1023–1027, https://doi.org/10.1038/nclimate3114, 2016.

Oishi, A. C., Hawthorne, D. A., and Oren, R.: Baseliner: An open-source, interactive tool for processing sap flux data from thermal dissipation probes, SoftwareX, 5, 139–143, https://doi.org/10.1016/j.softx.2016.07.003, 2016.

https://doi.org/10.5194/egusphere-2026-1881
Preprint. Discussion started: 18 May 2026

Oren, R., Sperry, J. S., Katul, G. G., Pataki, D. E., Ewers, B. E., Phillips, N., and Schäfer, K. V. R.: Survey and synthesis of intra- and interspecific variation in stomatal sensitivity to vapour pressure deficit, Plant Cell Environ., 22, 1515–1526, https://doi.org/10.1046/j.1365-3040.1999.00513.x, 1999.

Pappas, C., Matheny, A. M., Baltzer, J. L., Barr, A. G., Black, T. A., Bohrer, G., Detto, M., Maillet, J., Roy, A., Sonnentag, O., and Stephens, J.: Boreal tree hydrodynamics: asynchronous, diverging, yet complementary, Tree Physiol., 38, 953–964, https://doi.org/10.1093/treephys/tpy043, 2018.

Powell, T. L., Wheeler, J. K., de Oliveira, A. A. R., da Costa, A. C. L., Saleska, S. R., Meir, P., and Moorcroft, P. R.: Differences in xylem and leaf hydraulic traits explain differences in drought tolerance among mature Amazon rainforest trees, Glob. Change Biol., 23, 4280–4293, https://doi.org/10.1111/gcb.13731, 2017.

Scholz, F. G., Phillips, N. G., Bucci, S. J., Meinzer, F. C., and Goldstein, G.: Hydraulic Capacitance: Biophysics and Functional Significance of Internal Water Sources in Relation to Tree Size, in: Size- and Age-Related Changes in Tree Structure and Function, vol. 4, edited by: Meinzer, F. C., Lachenbruch, B., and Dawson, T. E., Springer Netherlands, Dordrecht, 341–361, https://doi.org/10.1007/978-94-007-1242-3_13, 2011.

Seabold, S. and Perktold, J.: Statsmodels: Econometric and Statistical Modeling with Python, 2010.

Sevanto, S., Ryan, M., Dickman, L. T., Derome, D., Patera, A., Defraeye, T., Pangle, R. E., Hudson, P. J., and Pockman, W. T.: Is desiccation tolerance and avoidance reflected in xylem and phloem anatomy of two coexisting arid-zone coniferous trees?, Plant Cell Environ., 41, 1551–1564, https://doi.org/10.1111/pce.13198, 2018.

Stoy, P. C., Katul, G. G., Siqueira, M. B. S., Juang, J.-Y., McCarthy, H. R., Kim, H.-S., Oishi, A. C., and Oren, R.: Variability in net ecosystem exchange from hourly to inter-annual time scales at adjacent pine and hardwood forests: a wavelet analysis, Tree Physiol., 25, 887–902, https://doi.org/10.1093/treephys/25.7.887, 2005.

Stoy, P. C., Richardson, A. D., Baldocchi, D. D., Katul, G. G., Stanovick, J., Mahecha, M. D., Reichstein, M., Detto, M., Law, B. E., Wohlfahrt, G., Arriga, N., Campos, J., McCaughey, J. H., Montagnani, L., Paw U, K. T., Sevanto, S., and Williams, M.: Biosphere-atmosphere exchange of CO_2 in relation to climate: a cross-biome analysis across multiple time scales, Biogeosciences, 6, 2297–2312, https://doi.org/10.5194/bg-6-2297-2009, 2009.

Sulman, B. N., Roman, D. T., Yi, K., Wang, L., Phillips, R. P., and Novick, K. A.: High atmospheric demand for water can limit forest carbon uptake and transpiration as severely as dry soil, Geophys. Res. Lett., 43, 9686–9695, https://doi.org/10.1002/2016GL069416, 2016.

Torrence, C. and Compo, G. P.: A Practical Guide to Wavelet Analysis, Bull. Am. Meteorol. Soc., 79, 61–78, https://doi.org/10.1175/1520-0477(1998)079%253C0061:APGTWA%253E2.0.CO;2, 1998.

Tyree, M. T. and Sperry, J. S.: Vulnerability of Xylem to Cavitation and Embolism, Annu. Rev. Plant Physiol. Plant Mol. Biol., 40, 19–36, https://doi.org/10.1146/annurev.pp.40.060189.000315, 1989.

Tyree, M. T. and Yang, S.: Water-storage capacity of Thuja, Tsuga and Acer stems measured by dehydration isotherms, 1990.

Vicente-Serrano, S. M., Peña-Angulo, D., Beguería, S., Domínguez-Castro, F., Tomás-Burguera, M., Noguera, I., Gimeno-Sotelo, L., and El Kenawy, A.: Global drought trends and future projections, Philos. Trans. R. Soc. Math. Phys. Eng. Sci., 380, 20210285, https://doi.org/10.1098/rsta.2021.0285, 2022.

Xia, Y., Sheffield, J., Ek, M. B., Dong, J., Chaney, N., Wei, H., Meng, J., and Wood, E. F.: Evaluation of multi-model simulated soil moisture in NLDAS-2, J. Hydrol., 512, 107–125, https://doi.org/10.1016/j.jhydrol.2014.02.027, 2014.